12WCEE 2000

SIMULATION OF NEAR FIELD SEISMIC GROUND MOTIONS BY FEM CONSIDERING SOURCE RUPTURE MECHANISM

Toshihiro TSUBOI[1] And Fusanori MIURA[2]

SUMMARY

We have developed a method to analyze fault rupture mechanism and to generate accompanying seismic waves based on a nonlinear finite element method. In this method, a fault is modeled by a series of joint elements of which constitutive relationships are based on the experiments on stick-slip shear failure of rock masses. We first investigated the relationship between source parameters such as distributions of stress drop and yield stress along a fault plane and the resulting rupture velocity and dislocation. Then we studied the relationship between the mesh size of the finite element model and frequency characteristics of simulated waves. And finally we discussed the validity of the proposed method by comparing the simulated motions obtained from the 1994 Northridge earthquake fault with the recorded ground motions. The following outcomes were obtained. (1) There was a linear relationship between the average dislocation and the average stress drop irrespective of the magnitude of initial stress and yield stress. (2) The average rupture velocity depended on the difference between the yield stress and the initial stress. The larger the difference, the smaller the average rupture velocity. (3) The simulated ground motions for the 1994 Northridge earthquake had similar amplitude, which implies the validity of the proposed method.

INTRODUCTION

The 1994 Northridge earthquake and the 1995 Hyogoken-Nanbu earthquake are the typical strong earthquakes that attached the highly civilized megalopolises. Lessons from these earthquakes emphasized the necessity and the importance of research on strong ground motions due to earthquakes that take place directly underneath large cities. Prior to these earthquakes, one of the authors has developed a simulation method to analyze fault rupture mechanism and to generate accompanying seismic waves based on a nonlinear finite element method [Toki and Miura, 1985]. In this method, a fault is modeled by a series of joint elements of which constitutive relationship was assumed to be simple elasto-plastic. Then we have modified the relationships based on the results from experiments on stick-slip shear failure of rock masses [Tsuboi and Miura, 1997].

The purposes of this study are, first, to investigate the relationship between source parameters such as the magnitude and distribution of stress drop and yield stress along a fault plane and the resulting rupture process such as the rupture velocity and distribution of dislocation. Then, to discuss the validity of our proposed method by comparing the observed accelerograms during the 1994 Northridge earthquake and simulated ones.

ANALYSIS METHOD

Modeling the fault and the governing equation of motion

The fault plane is modeled by a series of joint elements shown in Figure 1 that was first proposed to analyze fault rupture mechanism by Toki and Miura [1985]. The constitutive relationship was , however, assumed to be simple elasto-perfect plastic and they introduced fictitious shearing and normal joint springs to obtain the shear and normal stresses along the fault. We employed the constitutive relationships obtained from experiments on stick-slip shear failure of rock masses conducted by Ohnaka et al. [1987] for the constitutive relationship of the

[1] *Division of Design, Eirakukaihatsu Co. Ltd., 1-13-19 Yoshino, Higashi-ku, Nagoya, Japan*
[2] *School of Science and Engineering, Yamaguchi University, Tokiwadai, Japan E-mail: miura@earth.csse.yamaguchi-u.ac.jp*

joint element. The shearing joint spring, thus, has physical meaning. The schematic drawing of the relationship is shown in Figure 2. The relationship implies that the shear stress on the fault plane proportionally increases with the increment of relative displacement on the fault, and when the shear stress reaches the shear strength rupture occurs. After the occurrence of rupture, the shear stress exponentially decreases to the residual shear stress as shown in the figure. The stiffness matrix of the joint element is given by Equation (1).

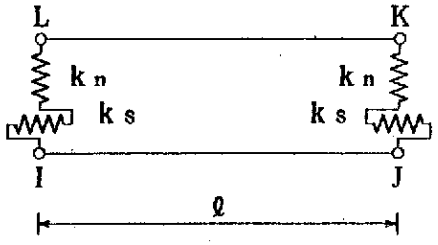

Figure 1: Schematic drawing of joint element

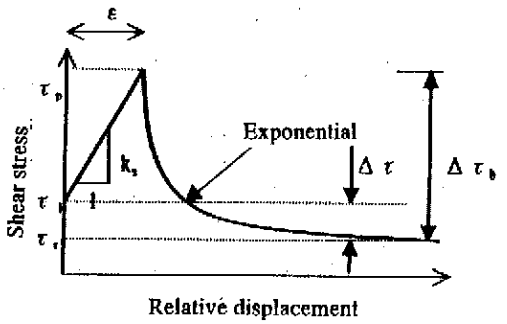

Figure 2: Constitutive relationship of the joint element

$$[K]_e = \frac{\ell}{2}\begin{bmatrix} ks & 0 & 0 & 0 & 0 & 0 & -ks & 0 \\ & kn & 0 & 0 & 0 & 0 & 0 & -kn \\ & & ks & 0 & -ks & 0 & 0 & 0 \\ & & & kn & 0 & -kn & 0 & 0 \\ & & & & ks & 0 & 0 & 0 \\ & & & & & kn & 0 & 0 \\ & Symm. & & & & & ks & 0 \\ & & & & & & & kn \end{bmatrix} \quad (1)$$

The analysis is basically a nonlinear analysis because sliding phenomenon along the fault plane is considered. The equation of motion, therefore, must be solved in the time domain. The load transfer method is employed to solve the nonlinear equation of motion, in which the stiffness matrix is kept constant throughout the analysis. The basic procedure of the dynamic analysis is described in previous papers [Toki and Miura, 1983 and Toki and Miura, 1985], but some procedures have been modified for the analysis of rupture on a fault plane as explained our previous paper[Tsuboi and Miura, 1996]. The equation of motion at time step *n* is written as;

$$\mathbf{[M]\{u\}_n + ([C] + [C^L] + [C^R] + [C^B])\{u\}_n + [K]\{u\}_n = \{F(n,s)\}} \quad (2)$$

in which **[M]**, **[C]**, **[K]** are the mass, damping and stiffness matrices of the system, $\mathbf{[C^L]}$, $\mathbf{[C^R]}$, $\mathbf{[C^B]}$ are the viscous boundary matrices for the left, right and bottom boundaries, respectively. **{u}** is the displacement vector, and **{F(*n*,*s*)}**is the external force vector calculated from the dynamic stress drop; and *n* and *s* stand for time step and nodal pairs where fault rupture takes place, respectively.

PARAMETRIC STUDY ON FAULT RUPTURE MECHAMNISM

Analyzed fault model

First, for the purpose of parametric study, we analyzed an actual active fault of which source parameters are obtained. Figure 3 shows the finite element model of the fault and crust near the fault. The hypocenter is assumed to be at the depth of 13km and shown by □ in the figure. The rupture propagates upward from the source and stops at the depth of 1 km. The constants for the crust are given in Table 1 and the source parameters for the fault are listed in Table 2. The number of freedom of this model is 4344. Based on the recent studies in the field of earth science, we assumed that the distributions of stresses along the fault such as initial stress,τ_i, peak stress,τ_p, residual stress,τ_d, stress drop $\Delta\tau$ and dynamic stress drop $\Delta\tau_b$ (breakdown stress drop) to increase with the depth as shown in Figures 4(a) and (b). These figures show the case in which the stress drop is 62 bar. In the following parametric study, the magnitude of stress drop and dynamic stress drop are changed to examine the effect of them on the fault rupture process.

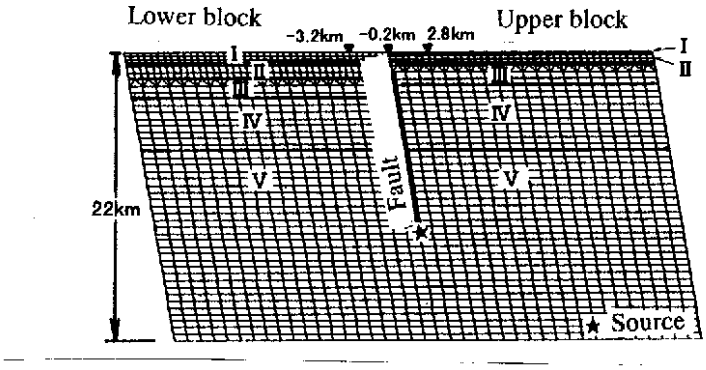

Figure 3: Finite element model of the fault and the vicinity

Table 1: Material constants of the crust model

Layer	Unit weight (tf/m^3)	P-wave velocity (km/s)	S-wave velocity (km/s)
I	1.9	1.9	0.6
II	2.1	3.0	1.5
III	2.3	5.0	2.8
IV	2.5	5.8	3.4
V	2.7	6.2	3.7

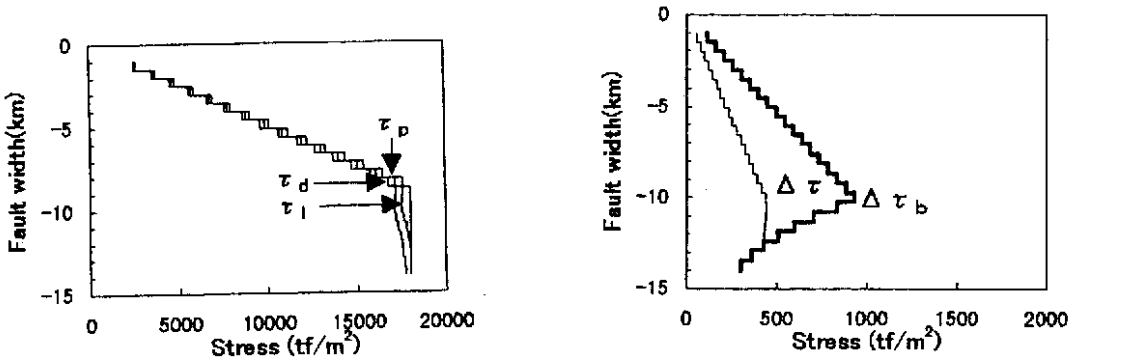

(a) Initial, τ_i, peak, τ_p, and residual, τ_d, stresses **(b) Stress drop $\Delta\tau$ and dynamic stress drop $\Delta\tau_1$**

Figure 4: Distribution of stresses along the fault

Table 2: Source parameters for the parametric analyses

Length L	20 km
Width W	13 km
Dip angle δ	80 degree
Slip direction λ	70 degree
Stress drop Δτ	60 bar
Magnitude M	7.0
Rupture velocity Vr	2.5 km/s
Dislocation U	160 cm

Analysis results

Figure 5 shows the relationship between the magnitude of stress drop and the average dislocations obtained from the parametric study. The magnitude of stress drop was parametrically changed from 30 bar to 120 bar. For each stress drop, the dynamic stress drop was varied. This result implies that the average dislocation is proportional to the stress drop alone irrespective of the magnitude of dynamic stress drop. It should be noted that the magnitude of dislocation shown in Table 2, which was probably obtained from the elastic dislocation theory is 160cm but the simulation results from our method are about 400cm as shown in Figure 5. This difference will be attributed to the existence of the free ground surface and the soft layer, and to two dimensional analysis approximation of three dimensional phenomenon.

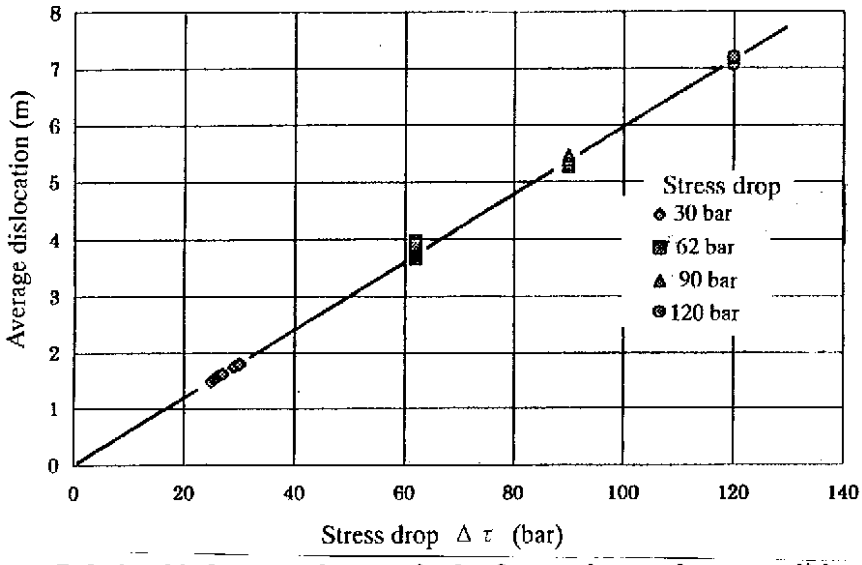

Figure 5: Relationship between the magnitude of stress drop and average dislocations

Figure 6 shows the relationship between the calculated average rupture velocity and dynamic stress drop. The average rupture velocities are larger than the S-wave velocity (about 3.5km/s) when the dynamic stress drop is small in the cases of the stress drop equals to 62, 90 and 120 bar, but they do not exceed the P-wave velocity (about 6km/s). The average rupture velocities gradually decrease as the dynamic stress drop increases. For the same dynamic stress drop, the average rupture velocity is faster for larger stress drop. When the dynamic stress drop is increased, the rupture finally ceases to propagate in the cases of the stress drop=30 and 62 bar. The same phenomenon will be obtained for the cases of the stress drop equals to 90 and 120 bar, if the dynamic stress drop is increased.

SIMURATION OF THE 1994 NORTHRIDGE EARTHQUAKE ACCELEROGRAMS

Analyzed fault model

In this chapter, we simulate the rupture process of the 1994 Northridge earthquake fault and obtain acceleration

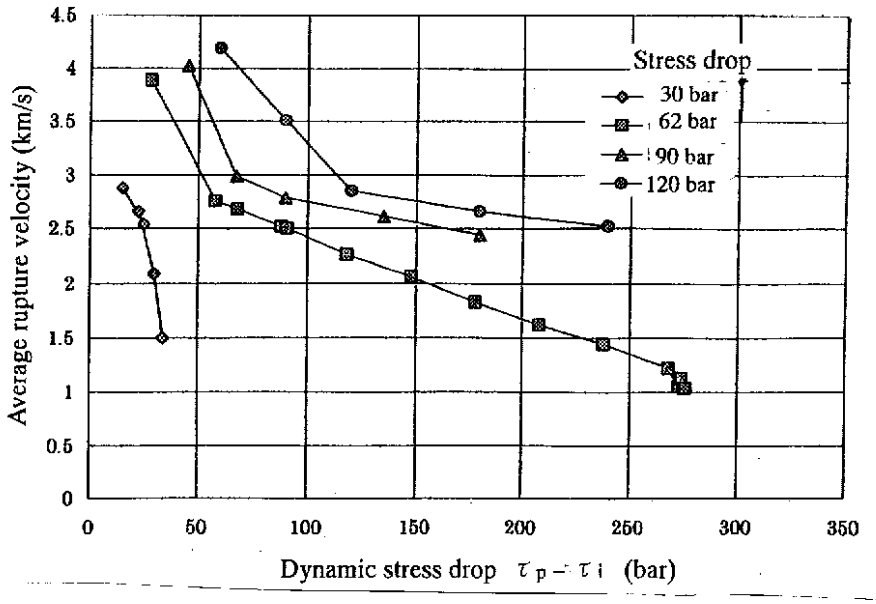

Figure 6: Relationship between the average rupture velocity and dynamic stress drop

time histories. We compare them with observed ones and discuss the validity of our method. Figure 7 shows the analyzed model and the corresponding crust constants are given in Table 3. The underground structure shown in Figure 7 and the constants in Table 3 were determined based on the previous work done by Pitarka and Irikura, [1994]. The number of freedom of the model is 13580. The source parameters of the fault are listed in Table 4 that were reported from Japan Society of Civil Engineers [1997]. We assumed the dynamic stress drop as 160 bar. In addition to this, we analyzed two more cases by changing the magnitude of stress drop, $\Delta\tau$, and dynamic stress drop $\Delta\tau_b$. These values are summarized in Table 5. The reason why we chose the values for Cases 2 and 3 is explained later. The distributions of stresses along the fault are assumed to be similar to those shown in Figure 4. The hypocenter is assumed to be at the depth of 13km and shown by ★ in the figure. The rupture propagates upward from the source and stops at the depth of 5 km. As can be seen from the figure, most part of the fault exists layers7, 8 and 9 and the average unit weight and shear wave velocity are 2.47 tf/m^3 and 3.64 km/s, respectively.

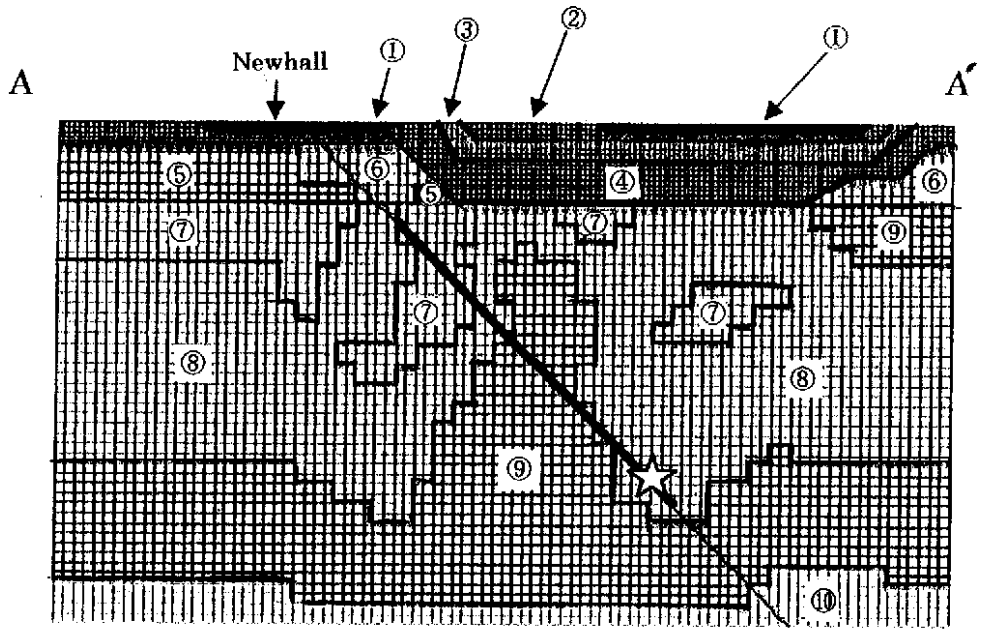

Figure 7: Analyzed fault model of the 1994 Northridge earthquake

Table 3: Material constants of the crust model

Layer	Unit weight (tf/m^3)	P-wave velocity (km/s)	S-wave velocity (km/s)
1	1.7	1.4	0.6
2	1.8	2.0	1.1
3	1.9	2.5	1.4
4	2.1	3.1	1.8
5	2.3	4.3	2.5
6	2.4	5.5	3.2
7	2.4	5.9	3.4
8	2.5	6.3	3.7
9	2.5	6.5	3.8
10	2.5	6.7	3.9

Table 4: Source parameters for the 1994 Northridge earthquake fault

Length L	13 km
Width W	20 km
Dip angle δ	45 degree
Stress drop $\Delta\tau$	74 bar
Magnitude M	6.8
Dislocation U	352 cm

Table 5: Assumed stress drop and dynamic stress drop

Case	Stress drop (bar)	Dynamic stress drop (bar)
1	74	160
2	55.3	141.3
3	46.1	132.1

Analysis results

The simulated average rupture velocities and dislocations are summarized in Table 6. The simulated average dislocation is 4.65m in Case 1and this is larger than the reported value of 3.52m. This difference is considered to be caused by the existence of free ground surface and by the two-dimensional analysis of three-dimensional phenomenon. Therefore, we tried to adjust the stress drop in the following manner. First, to compensate the effect of the free surface, we reduced the stress drop according to the ratio of the calculated dislocation, 4.65m, to the reported one, 3.52m, that is, 74 x 3.52 / 4.65 = 53.3 bar. This is the stress drop in Case 2. Next, to take into account the three-dimensional effect, we first obtain the dislocation, D, from the theoretical equation [Kanamori, H. 1982];

$$D=3\pi\Delta\tau a / (8\mu) \qquad (3)$$

By substituting the stress drop $\Delta\tau$=74 bar, the fault width, $2a$=20km, and $\mu=\rho Vs^2$, in which,ρ=2.47tf/m^3, Vs=3642m/s, into Eq.(3), we obtain D=2.90m. The stress drop used in Case3 is obtained in the same way as in Case 2. i.e., 74 x 2.90 / 4.63 = 46.1 bar. The resultant average dislocations for Cases 2and 3 are 3.55m and 3.00m

Table 6: Simulated average rupture velocities and average dislocations

Case	Average rupture velocity (km/sec)	Average dislocation (m)
1	3.10	4.65
2	2.97	3.55
3	2.88	3.00

We compare the observed accelerations at Newhall and simulated ones from Cases 1, 2 and 3. We applied high-cut filters of 2.2Hz and above to both the recorded horizontal and vertical accelerograms and simulated acceleration time histories in order to equate the frequency contents. Figure 8 shows the recorded and simulated time histories. Left figures are horizontal components and right figures vertical components, respectively. Figures (a) are observed accelerations and figures (b), (c) and (d) are from Cases 1, 2, and 3. The times in simulation are from the beginning of the analyses; therefore, the absolute time is not same as in the records.

First, we recognize that the duration of simulated time histories is longer than that of recorded ones. For horizontal components, the simulated maximum accelerations are smaller compared with that of observed one, but on the contrary, in vertical component, the recorded maximum acceleration is larger than simulated ones. Generally speaking, however, the magnitudes are on the same order, and this implies the validity of the simulation method.

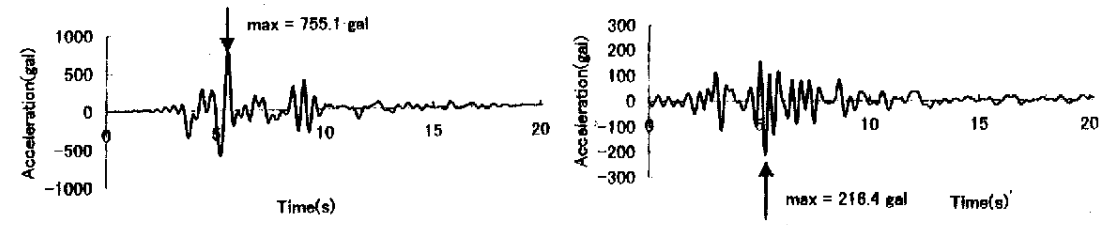

(a) Observed records

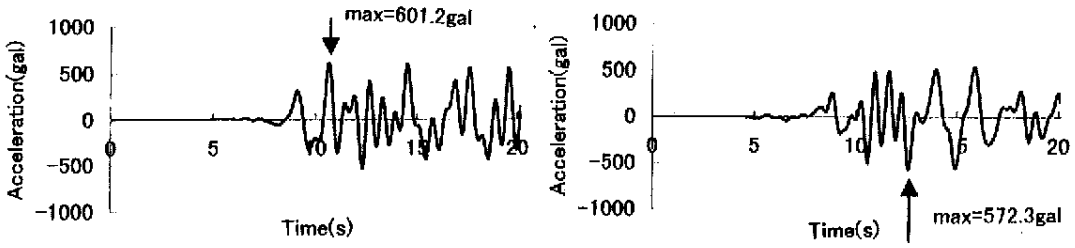

(b) Case1

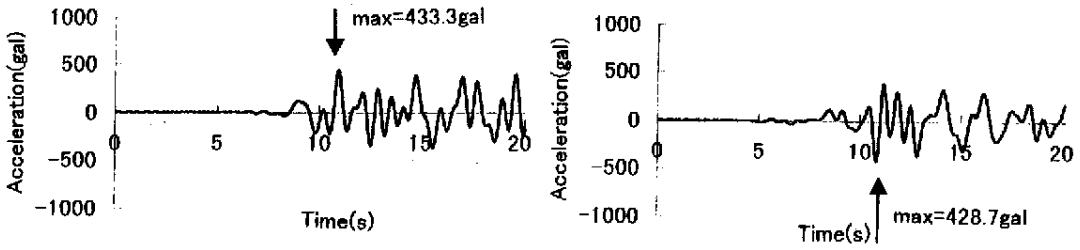

(c) Case 2

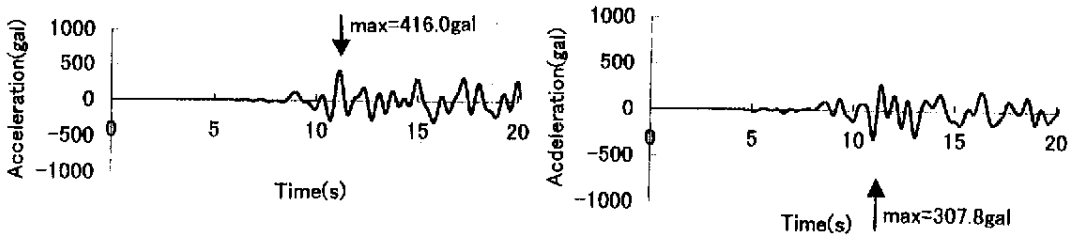

(d) Case 3

Figure 8: Comparison of observed and simulated acceleration time histories

CONCLUSION

By performing parametric study with different magnitude and distribution of stress drop, yield stress and initial stress along the fault, we could obtain the following outcomes.

(1) There was a linear relationship between the average dislocation and the average stress drop irrespective of the magnitude of initial stress and yield stress, that is, dynamic stress drop.

(2) The average rupture velocity depended on the difference between the yield stress and the initial stress. The larger the difference, the smaller the average rupture velocity. When the difference was small, the rupture velocity exceeded the S-wave velocity, but not the P-wave velocity.

(3) The simulated accelerations for the 1994 Northridge earthquake had similar magnitude of amplitude to the recorded motions, which implies the validity of the proposed method.

The obtained results were consistent with those from previous studies based on the elastic dislocation theory and observations done by others. However, the method is based on a two-dimensional finite element method, and the obtained results such as the magnitude of dislocation and ground motions are a little bit larger in calculation than those obtained from the elastic theory or recorded ones. We, therefore, need to develop a three dimensional analysis method to obtain more precise results.

REFERENCES

Ohnaka, M., Y. Kuwahara and K. Yamamoto (1987), "Constitutive relations between dynamic physical parameters near a tip of the propagating slip zone during stick-slip shear failure", *Tectonophysics*, 144, pp109-125.

Kanamori H. (1982), *Physics of the earthquake, Earth science 8*, Iwanami, pp74-76 (in Japanese).

Pitarka, A and K. Irikura (1994), "Basin structure effects on long-period strong motions in the San Fernando Valley and the Los Angels basin from the 1994 Northridge earthquake and an aftershock", *BSSA*, Vol.86, No.1B, pp126-137.

Toki, K. and F. Miura (1983), "Nonlinear seismic response of soil-structure interaction system", *Earthquake Engineering and Structural Dynamics*, 11, pp77-89.

Toki, K. and F. Miura (1985), "Simulation of a fault rupture mechanism by two-dimensional finite element method", *J. Phys. Earth*, Vol.33, pp485-511.

Tsuboi, T., and F. Miura (1996), "Simulation of stick-slip shear failure of rock masses by a nonlinear finite element method", *J. of structural mechanics and earthquake engineering*, JSCE, No.537/I-35, pp61-76, (in Japanese).